Electro-Osmotic Blood Flow of Shear-Thinning Fluid with Hall Current and Wall Flexibility

Anum Tanveer[1], Bushra Hameed[1], Tasawar Hayat[2,3], Ahmed Alsaedi[3]

[1]*Department of Mathematics, Mirpur University of Science and Technology (MUST), Mirpur Ajk 10250, Pakistan*
[2]*Department of Mathematic, Quaid-I-Azam University Islamabad, Islamabad 49000, Pakistan*
[3]*NAAM Research Group, Department of Mathematic, King Abdulaziz University, Jeddah 21589, Saudi Arabia*

Abstract

The presented article aims to present the flow of blood in microchannels such as veins and arteries via peristaltic flow. The magnetic field is imposed to regulate the flow as laminar. Also, its impacts in terms of Hall current have been considered. The rate of heat transfer is further based on Joule heating and viscous dissipation aspects. Mathematical analysis has been conducted given long wavelength and small Reynolds number. Such preferences are relatable to the medical domain where the magnetic field regulates the flow stream and aids in the melting of blood clots in patients with various heart diseases. The solution for electric potential is calculated analytically while the velocity, temperature, and heat transfer rate are executed directly via the built-in command of Mathematica software. Since the magnetic field acts as an opposing force. Results show that the velocity and temperature are decreasing functions of the magnetic field. However, the temperature is increasing for Weissenberg number.

Keywords: *Electro-Osmosis, Joule heating, Hall current, Magneto-hydrodynamics, Shear thinning fluid.*

1. Introduction

The recent past demonstrates that more attention has been paid to the field of study known as "microfluidics" in order to make improvements in micro fabrication technologies available. Electroosmotic flow (EOF) is important in a microfluidic system. Electroosmosis is essentially an electrokinetic process that investigates the ionic growth of fluids subjected to electric fields. A Stern layer (a charged surface with a high concentration of counter ions) is formed as a result of this action. The resulting Stern layer, combined with the diffusing layer, creates an Electric Double Layer (EDL). The potential (interfacial) between the diffuse double layer and the Stern layer is known as the zeta potential, and it is an important feature of many electrokinetic phenomena. Electrokinetic transportation has emerged as a vibrant area of modern fluid mechanics. Controlling biological transport systems requires an understanding of the combined effects of electrokinetic and peristaltic events. Electrokinetics includes electrophoresis, electroosmosis, diffusiophoresis, and other phenomena. Many microfluidic devices, including Lung chips, proteomic chips, lab-on-a-chip (LOC), portable blood analyzers, micro-peristaltic pumps, organ-on-a-chip, micro-electro-mechanical systems (MEMS), micro-peristaltic pumps, DNA and bioMEMS, and microscopic full analysis systems, are based on the EDL and electroosmosis ideologies. Furthermore, MEMS, automation and parallelization, cost-effectiveness analysis, integration, miniaturisation, separation, biological/chemical component investigation, and high efficiency advancement are all related to microfluidic devices. Bag and Bhattacharyya [1] investigated non-Newtonian fluid with electro-osmotic effect in a micro-channel. The topic addresses the streaming of an ionic fluid with an electric field operation that is perpendicular to the electric object. According to an ambient electrical field which induces displacement of solvent molecules through viscous pull, the ionic items in the powered control plate are forced to

Corresponding author: Anum Tanveer *(anum.maths@must.edu.pk)*
Received: *15 February 2013*; Revised: *26 July 2023*; Accepted: *4 August 2023*; Published: *11 September 2023*

move. Despite considerable developments in direct peristaltic flow modeling, comparatively less progress has been shown in growing peristaltic flow possibilities. One such illustration is micro flow analysis by incompressible magneto-hydrodynamic fluid [2]. Microfluidic is one of the most significant field of science that utilizes micro-electromechanical potential as a tool for the study of simple biochemical and physical mechanisms as well as a medium for biological and chemical processing. However, such electrical fields or electro-osmotic effects owing to peristaltic blood flow has not given much attention. J. Akram et al. [3], interestingly put forward an analysis to show the logical findings for the rate of movement of micro fluid particles in peristaltic flows. Hussain and Ali [4] examined the electro-kinetically moderated shear thinning transfer of fluids through a small divertible channel. They found the drastic results of electro-osmosis for the increase of pressure at lower concentration. Also the trapping is proficiently controlled by an electrical field and remains avoided at acceptably stronger electrical field power, as is the case with Hussain and Ali [4]. Further, Nekoubin [5] investigated power-law fluid's electro-osmotic effect for high zeta potentials in curved micro-channel. Nazeer et al. [6] numerically clarified the electro-osmotic behavior of non-Newtonian fluids. Zeeshan et al. [7] also examined the electro-osmotic transport through a rectangular peristaltic pump induced by complex traveling wave with zeta potential and heat source. Akram et al. [8] considered electro-kinetic transport of nanofluid. Some researchers study the electroosmotic flow of different elements in a microchannel [9-13]. Zeeshan et al. [14] study the Electroosmosis-modulated bio-flow of nanofluid through a rectangular peristaltic pump induced by complex traveling wave with zeta potential and heat source. Traditional liquids such as water and natural oil have been shown in the literature to fall short of meeting contemporary expectations for improved thermal conductivities. Nanofluid research is a hot issue right now since it improves the thermal conductivity of traditional liquids. The nanofluidic flow issue has several applications in biomedical engineering, including medication delivery utilizing nanoparticles, heat exchanges, and tumor treatment. However, scholars have paid close attention to all of the above phenomena. Due to its wide range of purposes in the clinical and industrial sectors, the magnetic field has gained importance. Maraj et al. [15] Menthol-based nanofluid electroosmotically controlled magnetohydrodynamic peristaltic flow in a uniform channel with shape factor. The shear rate for blood flow is less and so MHD can be helpful to control blood flow from stenosis the arteries during cardiac surgery in the field of medicine. When considering a strong magnetic field, Hall effects cannot be ignored. Some representative researches explaining MHD, Hall current and radiation can be used through references [16-21]. Reddy and Reddy [22] studied the peristalsis of the MHD fluid in a porous medium.

Blood is measured as non-Newtonian liquid (at low shear rate), especially near the dimension of cell. Suspended substances, as cells in blood are the source of non-Newtonian behavior. Shot et al. [23] implemented a model in which blood is treated through equations of viscoelastic material. Here research is restricted to the transmission of harmonic waves with low amplitude and the calculations are limited to mild stenosis. The observations discussed to indicate only improvements in the separate area, velocity distribution, confrontation, and wall shear stress, there is no proof of the effect of stenosis on strain and streamlines. There is still plenty more to be observed in the case of stenosis with the combined consequences of endogenous shear thinning flow and blood characteristics. Faster processors and further sophisticated computational procedures have at this instant made it conceivable to use a better network and in further realistic conditions to carry out studies. References [24-26] show some relevant revisions on non-Newtonian blood flow. Power law fluid is the simplest non-Newtonian material. It determines the thickening and thinning of the substance. Nevertheless, the major drawback is that at very low and very high shear levels it is effectual. The Carreau fluid model was therefore proposed to address this drawback. Work in pulsatile flow of non-Newtonian fluid is vast, rather than electro-osmotic aspects it is very limited. Hayat et al. [27] examined the magneto-hydrodynamic effect on peristalsis of shear thinning fluid in a channel. Noreen et al. [28] studied Carreau fluid in a curved channel for peristaltic motion. Tanveer et al. [29] examined peristaltic flow of Carreau fluid in a curved channel.

In arterial blood flow processes, the channel walls (arteries and veins) are usually flexible. However, most of the research on the topic uses the fixed pressure assumption and less focus has been given to wall flexibility properties. Bhatti et al. [30] study heat transfer

analysis and effect of Hall current on peristaltic activity with flexible walls. Gudekote et al. [31] elaborated wall flexibility impact on peristaltic flow through an inclined non-uniform channel. Gudekote et al. [32] also considered impact of wall properties conditions for non-Newtonian fluid in a non-uniform channel. Eldesoky et al. [33] interpreted the impacts of flexibility of walls and slip conditions on peristalsis in the presence of heat transfer analysis.

Motivated by above mentioned aspects, this research has been designed to examine the peristaltic blood flow in arteries with magnetic field. Non-Newtonian liquid exhibiting shear thinning is taken, Hall current is retained. The considered problem has been simplified for long wavelength assumption and then solved for series solutions. The effects of pertinent parameters are described in detail in last section.

2. Mathematical expressions

2.1. Regime of flow

Electro-osmotic flow of two-dimensional incompressible shear thinning fluid in a micro channel having width 2D is considered. The wave propagation is along ξ-axis and η-axis transverse to ξ-axis. The flexible walls are for channel are taken (see Figure 1).

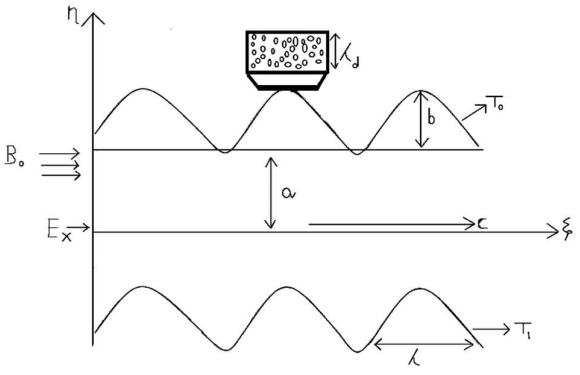

Figure 1. Geometry of the problem.

The stronger magnetic field (0, 0, B_0) is added with Hall current effect and it maintains Joule heating. Peristaltic waves travel along compliant walls of micro channel. The geometric model for the electro-osmotic shear thinning blood flow along complaint walls and an axially applied electric field, E_ξ is follows.

Mathematical the wave shape is described by [7]:

$$\pm\hat{h} = \pm[a - b\sin\frac{2\pi}{\lambda}(\hat{\xi} - c\hat{t})] \tag{1}$$

Where $\pm h, a, b, \lambda, \hat{\xi}, c, \hat{t}$ represent the displacement of upper and lower walls, the half width at the inlet, wave amplitude, wavelength, axial coordinate, wave velocity and time respectively. The electrical field retains only the component of axial electrical field, and $E\xi$, Electric field generation is emitted since we are supposing electro-kinetic flow rather than electro-hydrodynamic (EHD) movement. In the following electrical areas, because of the low thermal conductivity of fluids used in EHD, they are broad enough to produce electrical induction phenomenon. Moreover, they are not mentioned in electro-kinetic flow.

Applied magnetic field is expressed as [16]:

$$\hat{B} = (0, 0, \boldsymbol{B}_0). \tag{2}$$

Current density satisfies [16]:

$$\hat{J} = \frac{\sigma}{1+\alpha^2}[(\hat{V} \times \hat{B}) - \frac{1}{en}(\hat{J} \times \hat{B})]. \tag{3}$$

Lorentz force $\hat{F} = \hat{J} \times \hat{B}$ leads to

$$\hat{J} \times \hat{B} = -\frac{\sigma \boldsymbol{B}_0^{\,2}}{1+\alpha^2}[(\hat{u} - \alpha\hat{v}), \hat{v} + \alpha\hat{u}, 0], \tag{4}$$

where $\hat{J}$ represents the current density, $\hat{V}$ velocity, e charge on electron, n density of electron numbers, $\hat{u}$ and $\hat{v}$ velocity variables in $\hat{\xi}$ and $\hat{\eta}$ directions, $\boldsymbol{B}_0$ magnetic field strength, $\alpha = \frac{\sigma \boldsymbol{B}_0}{en}$ the Hall current parameter and σ electric conductivity of fluid.

2.2. Shear thinning fluid model

Cauchy stress tensor for Shear Thinning fluid obeys [34]:

$$\hat{\tau} = \mu(\hat{\dot{\gamma}})\hat{A}_1 \tag{5}$$

with

$$\hat{\tau} = -\left[\mu_\infty + (\mu_0 - \mu_\infty)(1 + \Gamma\hat{\gamma})^{\frac{n-1}{2}}\right]\hat{\gamma}, \quad (6)$$

$$\hat{A}_1 = \nabla\hat{v} + \nabla\hat{v}^T, \quad (7)$$

where $\hat{\tau}$ denotes extra stress tensor, μ_∞ infinite shear rate viscosity, μ_0 zero shear rate viscosity, Γ the time constant, n fluid index and $\hat{\dot{\gamma}}$ is expressed as

$$\hat{\dot{\gamma}} = \sqrt{\frac{1}{2}\sum_i\sum_j \hat{\dot{\gamma}}_{ij}\hat{\dot{\gamma}}_{ji}} = \sqrt{\frac{1}{2}\Pi} = \sqrt{\frac{1}{2}tr\hat{A}_1^2}. \quad (8)$$

Here Π is second invariant stress tensor. We take the case for which $\mu_\infty = 0$ and $\Gamma\hat{\dot{\gamma}} < 1$. Thus

$$\hat{\tau} = -\mu_0[1 + (\tfrac{n-1}{2})\Gamma^2\hat{\dot{\gamma}}^2]\hat{\dot{\gamma}}. \quad (9)$$

2.3. Distribution of electric potential:

Poisson expression for electrical potential is used as a consequence of the existence of EDP in the micro channel satisfying [28].

$$\nabla^2\hat{\Phi} = -\frac{\hat{\rho}_e}{\epsilon\epsilon_0}. \quad (10)$$

Here ρ_e depicts density of total ionic change, ∈ relative permittivity of the medium and ϵ_0 permittivity of free space. Density of total ionic energy in a symmetric electrolyte, ρ_e satisfies, $\rho_e = -ez(n^+ - n^-)$, where n^+ and n^- elucidate the density numbers of Poisson equation for cations and anions can be described by.

$$\hat{n}^{\pm} = \hat{n}_0 e^{(\pm\frac{ez}{T_{av}K_B}\hat{\Phi})}. \quad (11)$$

Where $n_0, e, z, T_{av}, and\ K_B$ are the number density/bulk concentration, electronic charge, charge balance, average temperature, and Boltzmann constant.

Nernst-Planck expression is established to evaluate the distribution for potential and defines the density of charge number i.e.

$$\frac{\partial\hat{n}_\pm}{\partial\hat{t}} + (q.\nabla)\hat{n}_\pm = D\nabla^2\hat{n}_\pm \pm \frac{Dze}{K_BT}\left(\nabla.\left(\hat{n}_\pm\nabla\hat{\Phi}\right)\right). \quad (12)$$

Further $Sc = \frac{\mu}{\rho_f.D}$, $\varphi = \pm\frac{ez}{T_{av}K_B}\hat{\Phi}$ represents the Schmidt number, non-dimensional electroosmotic parameter φ and $P\,e = Re.Sc$ denotes ionic Peclet number. Poisson equation is obtained by using limits $Re, Pe, \delta \ll 1$ as follows:

$$\frac{\partial^2\varphi}{\partial\eta^2} = \kappa^2\left(\frac{n_+ - n_-}{2}\right). \quad (13)$$

And Nernst Planck expression is of the form:

$$0 = \frac{\partial^2 n_\pm}{\partial\eta^2} \pm \frac{\partial}{\partial\eta}\left(n_\pm\frac{\partial\varphi}{\partial\eta}\right). \quad (14)$$

Bulk conditions for equation are

$$n_\pm(\varphi = 0) = 1, \frac{\partial n_\pm}{\partial\eta}\left(\frac{\partial\varphi}{\partial\eta} = 0\right) = 0. \quad (15)$$

Now, first simplifying the Equation (23) subject to the boundary conditions mentioned in Equation (24). This gives the ionic Boltzmann distribution as follows:

$$n_\pm = e^{\pm\Phi}. \quad (16)$$

The Poisson–Boltzmann function is obtained as:

$$\frac{\partial^2\varphi}{\partial\eta^2} = m^2 sinh\varphi. \quad (17)$$

Where $m = aez\sqrt{\frac{2n_0}{\varepsilon K_B T}} = \frac{a}{\lambda_d}d$, $\lambda_d = \frac{1}{ez_v}\sqrt{\frac{T_0\epsilon K_B}{2n_0}}$, are parameter sof electroosmosis and λ_d Debye length.

A low-zeta potential technique must be used to modify Equation (38). Using Debye-Huckel approximation i.e., $sinh\varphi \approx \varphi$.

Now equation (17) becomes

$$\frac{\partial^2\varphi}{\partial\eta^2} = m^2\varphi. \quad (18)$$

Implementing boundary conditions $\frac{\partial\varphi}{\partial\eta}(0) = 0$ and $\varphi(h) = 1$, whereas the analytical solution of electric potential Φ is obtained

$$\varphi = \frac{coshm\eta}{coshmh}. \quad (19)$$

2.4. Governing equations

Suppose the electro-osmotic blood flow of an incompressible shear thinning fluid by use of an externally distributed electric field. Energy expression is

supposed with viscous dissipation. Relevant expressions obey [28]:

$$\frac{\partial \hat{u}}{\partial \hat{\xi}} + \frac{\partial \hat{v}}{\partial \hat{\eta}} = 0, \tag{20}$$

$$\rho\left(\frac{\partial \hat{u}}{\partial \hat{t}} + \hat{u}\,\frac{\partial \hat{u}}{\partial \hat{\xi}} + \hat{v}\frac{\partial \hat{u}}{\partial \hat{\eta}}\right) = -\frac{\partial \hat{p}}{\partial \hat{\xi}} + \frac{\partial \hat{\tau}_{\hat{\xi}\hat{\xi}}}{\partial \hat{\xi}} + \frac{\partial \hat{\tau}_{\hat{\xi}\hat{\eta}}}{\partial \hat{\eta}} - \frac{\sigma {B_0}^2}{1+\alpha^2}(\hat{u} - \alpha\hat{v}) + \hat{\rho}_e E_\xi, \tag{21}$$

$$\rho\left(\frac{\partial \hat{v}}{\partial \hat{t}} + \hat{u}\,\frac{\partial \hat{v}}{\partial \hat{\xi}} + \hat{v}\frac{\partial \hat{v}}{\partial \hat{\eta}}\right) = -\frac{\partial \hat{p}}{\partial \hat{\eta}} + \frac{\partial \hat{\tau}_{\hat{\eta}\hat{\xi}}}{\partial \hat{\xi}} + \frac{\partial \hat{\tau}_{\hat{\eta}\hat{\eta}}}{\partial \hat{\eta}} - \frac{\sigma {B_0}^2}{1+\alpha^2}(\hat{v} + \alpha\hat{u}), \tag{22}$$

$$\rho c_p\left(\frac{\partial T}{\partial \hat{t}} + \hat{u}\,\frac{\partial T}{\partial \hat{\xi}} + \hat{v}\frac{\partial T}{\partial \hat{\eta}}\right) = k\left(\frac{\partial^2 T}{\partial \hat{\xi}^2} + \frac{\partial^2 T}{\partial \hat{\eta}^2}\right) + \frac{\sigma \boldsymbol{B_0}^2}{1+\alpha^2}(\hat{u}^2 + \hat{v}^2) + \left[\left(\frac{\partial \hat{u}}{\partial \hat{\eta}} + \frac{\partial \hat{v}}{\partial \hat{\xi}}\right)\right]\hat{\tau}_{\hat{\xi}\hat{\eta}} + \frac{\partial \hat{u}}{\partial \hat{\xi}}(\hat{\tau}_{\hat{\xi}\hat{\xi}} - \hat{\tau}_{\hat{\eta}\hat{\eta}})]. \tag{23}$$

In which $\hat{u}, \hat{v}, \hat{\xi}, \hat{\eta}, \rho, \hat{p}, \mu_0, T, k$ and E_ξ are axial velocity, transverse velocity, axial coordinate, transverse coordinate, fluid density, pressure, fluid viscosity, temperature, thermal conductivity and axial electrical field.

The relevant equation of motion for compliant walls as follows [33]:

$$M^* = \hat{p} - \hat{p}_0. \tag{24}$$

In which the operator M^* that describes the use for extended membrane movement with damping viscosity forces [33]

$$M^* = -\kappa\frac{\partial^2}{\partial \hat{\xi}^2} + l_1\frac{\partial^2}{\partial \hat{t}^2} + D\frac{\partial}{\partial \hat{t}}. \tag{25}$$

Here κ denotes membrane elastic tension, l_1 the mass, D coefficient of viscous damping forces and wall flexibility is:

$$\frac{\partial M^*}{\partial \hat{t}} = \frac{\partial \hat{p}}{\partial \hat{\xi}} = \frac{\partial \hat{\tau}_{\hat{\xi}\hat{\xi}}}{\partial \hat{\xi}} + \frac{\partial \hat{\tau}_{\hat{\xi}\hat{\eta}}}{\partial \hat{\eta}} - \rho\left(\frac{\partial \hat{u}}{\partial \hat{t}} + \hat{u}\,\frac{\partial \hat{u}}{\partial \hat{\xi}} + \hat{v}\frac{\partial \hat{u}}{\partial \hat{\eta}}\right) - \frac{\sigma \boldsymbol{B_0}^2}{1+\alpha^2}(\hat{u} - \alpha\hat{v}) + \hat{\rho}_e E_\xi. \tag{26}$$

We shall implement the following non-dimensional transformations [34, 35].

$$\xi = \frac{\hat{\xi}}{\lambda}, \eta = \frac{\hat{\eta}}{a}, t = \frac{c\hat{t}}{\lambda}, u = \frac{\hat{u}}{c}, v = \frac{\hat{v}}{c\delta}, p = \frac{\hat{p}a^2}{\mu_0 c\lambda}, \tau_{\xi\xi} = \frac{\lambda}{\mu_0 c}\hat{\tau}_{\hat{\xi}\hat{\xi}}, \tau_{\xi\eta} = \frac{a}{\mu_0 c}\hat{\tau}_{\hat{\xi}\hat{\eta}}, \tag{27}$$

$$\tau_{\eta\eta} = \frac{\lambda}{\mu_0 c}\hat{\tau}_{\hat{\eta}\hat{\eta}}, , h = \frac{\hat{h}}{a}, We = \frac{\Gamma c}{a}, M^2 = \frac{\sigma {B_0}^2}{\varepsilon(1+a^2)}, u = \psi_\xi, v = \psi_\eta, Re = \frac{\rho c a}{\mu_0}, \epsilon = \frac{b}{a}, \tag{27}$$

$$\delta = \frac{a}{\lambda}, Pr = \frac{\mu_0 c_p}{k}, E = \frac{c^2}{c_p(T_1 - T_0)}, Br = Pr.E, \hat{E}_1 = -\frac{\tau a_1^3}{\lambda^3 \mu c}, \hat{E}_2 = \frac{m_1 a_1^3 c}{\lambda^3 \mu}, \hat{E}_3 = \frac{a a_1^3}{\lambda^2 \mu}, \quad U_{HS} = -\frac{E_\xi \epsilon}{c\mu_0} \tag{28}$$

Where δ symbolize wave number, Re the Reynolds number, ϵ amplitude ratio parameter, $\hat{E}_1$ and $\hat{E}_2$ elastic parameters, $\hat{E}_3$ damping variable, ψ the stream function, M Hartmann number, We Weissenberg number, Pr the Prandtl number, E the Ercket number and Br the Brinkmann number. Now the related expressions satisfy

$$\frac{\partial u}{\partial \xi} + \frac{\partial v}{\partial \eta} = 0, \tag{29}$$

$$Re\delta\left[\frac{\partial u}{\partial t} + u\frac{\partial u}{\partial \xi} + v\frac{\partial v}{\partial \eta}\right] = -\frac{\partial p}{\partial \xi} + \delta^2\frac{\partial \tau_{\xi\xi}}{\partial \xi} + \frac{\partial \tau_{\xi\eta}}{\partial \eta} - M^2(u - \alpha\delta v) + m^2\varphi U_{HS}, \tag{30}$$

$$Re\delta^3\left[\frac{\partial v}{\partial t} + u\frac{\partial v}{\partial \xi} + v\frac{\partial v}{\partial \eta}\right] = -\frac{\partial p}{\partial \eta} + \delta^2(\frac{\partial \tau_{\eta\xi}}{\partial \xi} + \frac{\partial \tau_{\eta\eta}}{\partial \eta}) - M^2(v - \alpha\delta u) + m^2\varphi U_{HS}, \tag{31}$$

$$Re\delta Pr\left[\frac{\partial \theta}{\partial t} + u\frac{\partial \theta}{\partial \xi} + v\frac{\partial \theta}{\partial \eta}\right] = \delta^2\left(\frac{\partial^2 \theta}{\partial \xi^2} + \frac{\partial^2 \theta}{\partial \eta^2}\right) + Br\left[\left(\delta^2\frac{\partial v}{\partial \xi} + \frac{\partial u}{\partial \eta}\right)\tau_{\xi\eta} + \delta^3\frac{\partial u}{\partial \xi}(\tau_{\xi\xi} - \tau_{\xi\eta})\right] + M^2 Br(\delta^2 v^2 + u^2). \tag{32}$$

Where

$$\tau_{\xi\xi} = 2\delta\left[1 + \frac{n-1}{2}We^2\,\dot{\gamma}^2\right]\frac{\partial u}{\partial \xi}, \tag{33}$$

$$\tau_{\xi\eta} = \left[1 + \frac{n-1}{2}We^2\dot{\gamma}^2\right]\left(\frac{\partial u}{\partial \eta} + \delta^2\frac{\partial v}{\partial \xi}\right), \tag{34}$$

$$\tau_{\eta\eta} = 2\delta\left[1 + \frac{n-1}{2}We^2\dot{\gamma}^2\right]\frac{\partial v}{\partial \eta}. \tag{35}$$

$$\dot{\gamma} = \sqrt{\frac{1}{2}\delta\left(\left(\frac{\partial u}{\partial \xi}\right)^2 + \left(\frac{\partial v}{\partial \eta}\right)^2\right) + \left(\frac{\partial u}{\partial \eta} + \delta^2\frac{\partial v}{\partial \xi}\right)^2}. \quad (36)$$

Low Reynolds and long wavelength yield.

$$\frac{\partial p}{\partial \xi} = \frac{\partial}{\partial \eta}\left[1 + \frac{(n-1)}{2}We^2\left(\psi_{\eta\eta}\right)^2\right] - M^2\psi_\eta + m^2\varphi U_{HS}, \quad (37)$$

$$\frac{\partial p}{\partial \eta} = 0, \quad (38)$$

$$\frac{\partial^2 \theta}{\partial \eta^2} + Br\left[1 + \frac{(n-1)}{2}We^2\left(\psi_{\eta\eta}\right)^2\right]\left(\psi_{\eta\eta}\right)^2 + BrM^2(\psi_{\eta\eta})^2 = 0, \quad (39)$$

$$\frac{\partial}{\partial \eta}\left[1 + \frac{(n-1)}{2}We^2\left(\psi_{\eta\eta}\right)^2\right] - M^2\psi_\eta + m^2\varphi U_{HS} = \hat{E}_1\frac{\partial^3 h}{\partial \xi^3} + \hat{E}_2\frac{\partial^3 h}{\partial \xi \partial t^2} + \hat{E}_3\frac{\partial^2 h}{\partial \xi \partial t}, \quad (40)$$

$$\tau_{\xi\xi} = 0, \ \ \tau_{\eta\eta} = 0, \quad (41)$$

$$\tau_{\xi\eta} = -\left[1 + \frac{(n-1)}{2}We^2\left(\psi_{\eta\eta}\right)^2\right]\psi_{\eta\eta}. \quad (42)$$

And incompressibility constraint is satisfied. Non-dimensional form of coefficient of heat transfer is described as:

$$z = h_\xi \theta_\eta. \quad (43)$$

2.5. Boundary conditions

The significance of velocity and temperature at the walls of the micro channel are given by [22]

$$T = T_0 \ at \ \hat{\eta} = -\hat{h}, \quad (44)$$

$$T = T_1 \ at \ \hat{\eta} = \hat{h}, \quad (45)$$

Where T_0 and T_1 depict the temperature on the top and bottom walls of micro channel and T implies the temperature.

The boundary conditions are described as follows [35].

$$u = 0 \ at \ \eta = -h.h \implies \psi_\eta = 0 \ at \ \eta = -h.h, \quad (46)$$

$$\hat{E}_1\frac{\partial^3 h}{\partial \xi^3} + \hat{E}_2\frac{\partial^3 h}{\partial \xi \partial t^2} + \hat{E}_3\frac{\partial^2 h}{\partial \xi \partial t} = \delta^2\frac{\partial \tau_{\xi\xi}}{\partial \xi} + \frac{\partial \tau_{\xi\eta}}{\partial \eta} - Re\delta\left[\frac{\partial u}{\partial t} + u\frac{\partial u}{\partial \xi} + v\frac{\partial u}{\partial \eta}\right] + M^2(u - \alpha\delta v) + m^2\varphi U_{HS}, \quad (47)$$

$$\theta = 0 \ at \ \eta = -h \ and \ \theta = 1 \ at \ \eta = h. \quad (48)$$

3. Results and discussion

The obtained system of equations is highly non-linear whose exact solutions seems impossible to find. Hence the problem in hand is executed numerically via built-in software NDSolve in Mathematica. Such technique provides graphical description directly and thus complicated solution terms are avoided. The key point is to investigate effects of relevant parameters on significance of velocity contribution, significance of temperature contribution, coefficient of heat transfer and stream lines.

The numerical and analytical findings inside this section are presented via the graphs. Figures-2((a)-(e)), Figures 3((a)-(e)) and Figures 4((a)-(e)) show numerical findings and some significant data which has been obtained through ND Solve by using Mathematica.

3.1. Velocity distribution

This subsection uses Figures 2 ((a)-(e)) to show how velocity changes in response to changes in the various related parameters. These figures examine the significance of velocity contribution under the influences of electro-osmotic parameter m, Hartmann number M, Helmholtz-Smoluchowski velocity U_{HS}, Weissenberg number We and fluid index n.

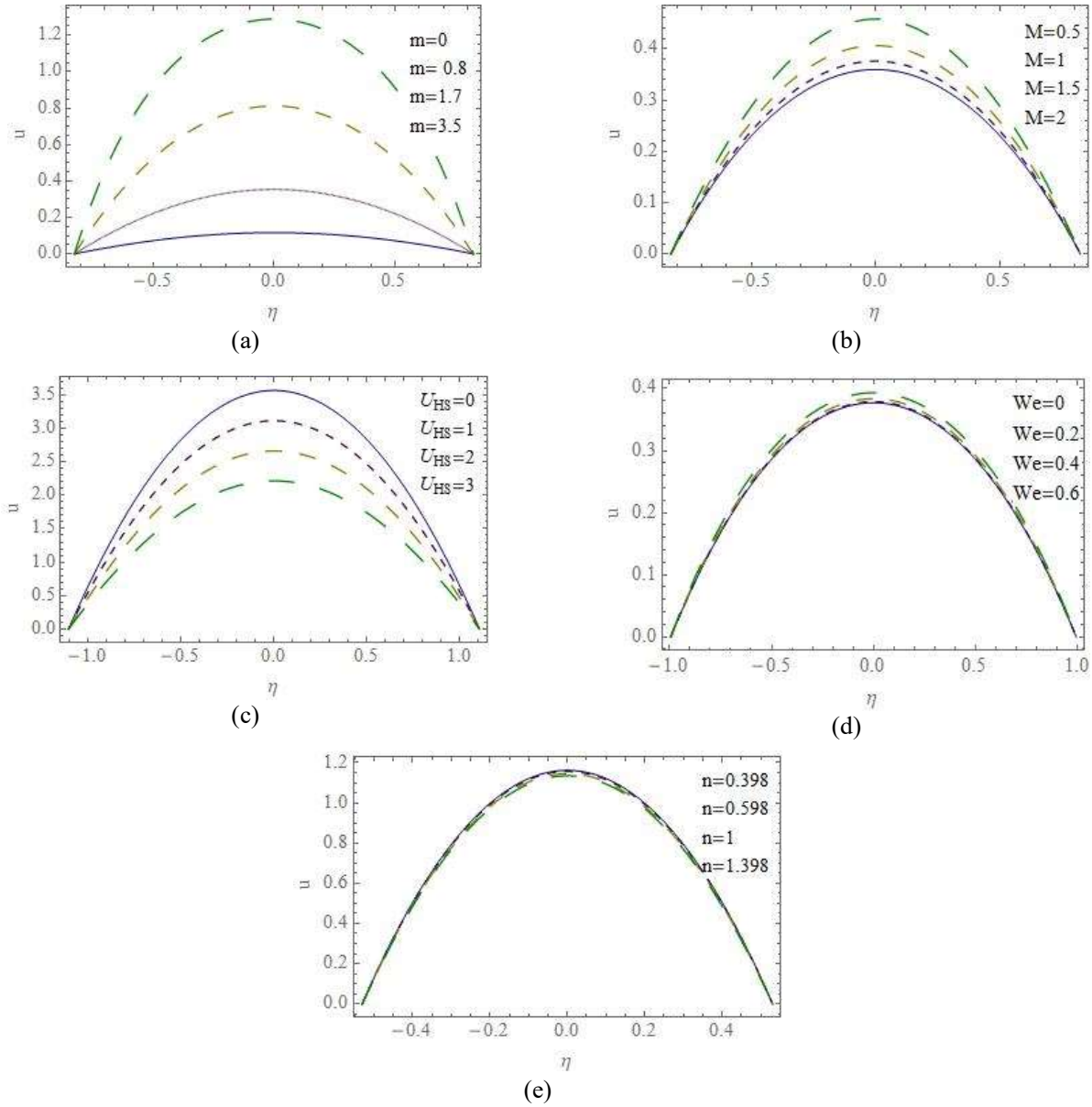

Figure 2. Significance of velocity contribution u for (a). m (b). M (c). U_{HS} (d). We (e) n, while other parameters are. $\xi = 1, t = 0.1, \epsilon = 0.8, \phi = 0.2, \hat{E}_1 = 0.1, \hat{E}_2 = 0.2, \hat{E}_3 = 0.1, m = 1,\ n = 0.398, M = 0.9, Br = 2,\ U_{HS} = -1, We = 0.07.$

Figure 2(a) shows that m improves strength of u, that is, the velocity u increases through higher m in the middle of channel. Since m is the fraction of the conduit height to theλ_d, it signifies that the increase of λ_d leads to a decrease in EDL, so that a large amount of fluid rapidly flows in the central region. In fact, for larger values of m the effective conductivity decreases. It causes decrease in magnetic damping force and hence axial velocity enhances. Figure 2(b) indicates that u increases when M enhances. As M is the fraction of Lorentz force (electromagnetic force) to viscous force, higher values of Hartmann number indicate stronger Lorentz force, hence more pressure is needed to overcome the Lorentz force. Figure 2(c) reveals that u decreases in the channel center with larger U_{HS} whreas contrary behavior is examined near wall. In fact, U_{HS} interprets physically the fluid speed decreases with higher EDL thickness. Figure 2(d) estimated that u enhances with an increase in We. Figure 2(e) predicted that u decreases with higher n. We noted that our analysis is compatible with previous results presented in references [35, 36].

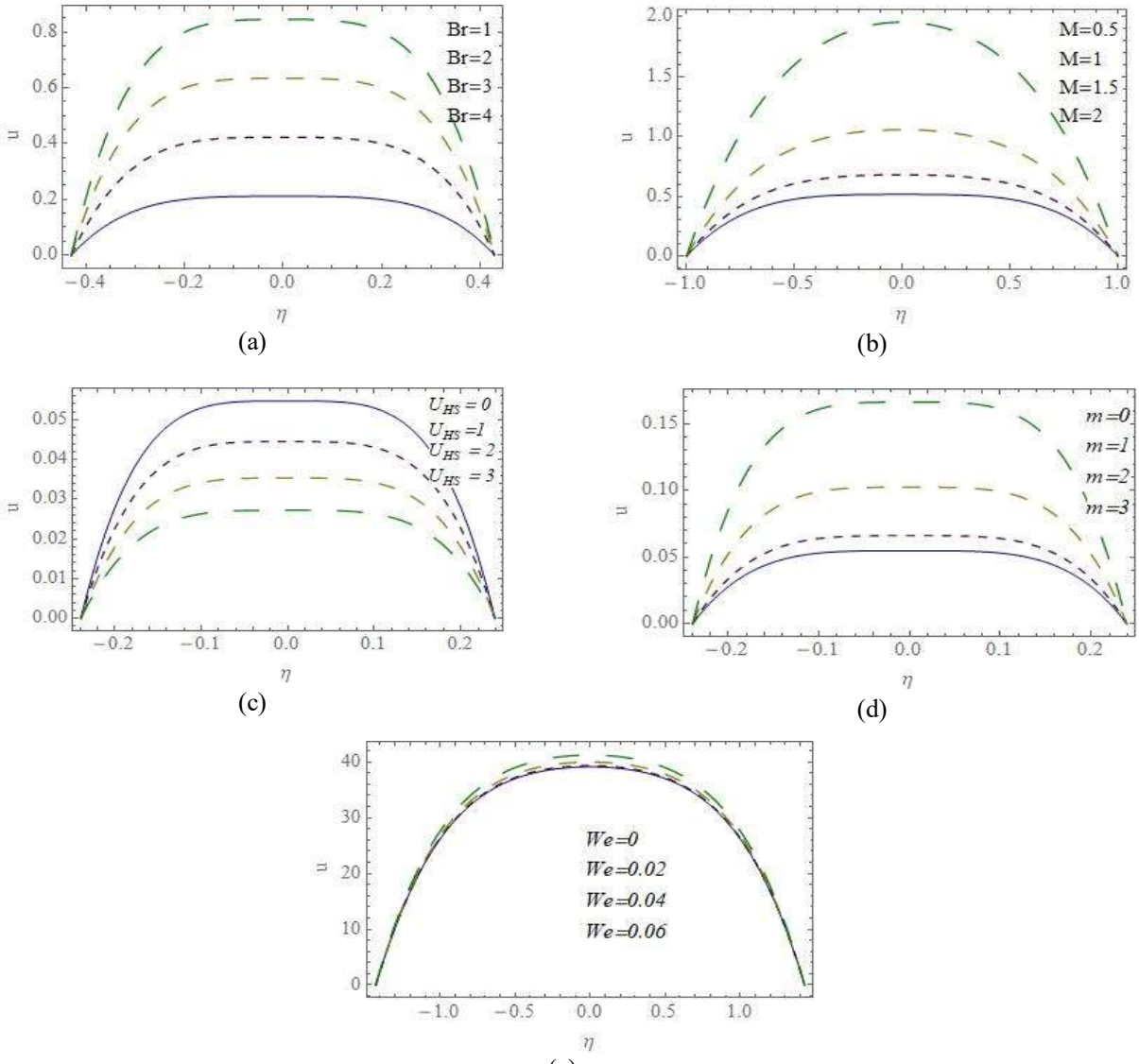

Figure 3. Significance of temperature contribution θ for (a). Br (b). M (c). U_{HS} (d). m (e) We, while other parameters are. $\xi = 0.1, t = 0.4, \epsilon = 0.3, \phi = 0.2, \hat{E}_1 = 0.1, \hat{E}_2 = 0.2, \hat{E}_3 = 0.1, m = 1,\ n = 0.398, M = 0.9, Br = 2,\ U_{HS} = -1, We = 0.05.$

3.1. Temperature distribution

The figures 3 ((a)-(e)) interprets the significance of temperature contribution under the impacts of Brinkmann number Br, Hartmann number M, Helmholtz-Smoluchowski velocity U_{HS}, parameter of electro-osmotic m and Weissenberg number We.

Figure-3(a) shows the effects of Br on θ, i.e., θ increases for higher Br values, since Br describes the viscous dissipation which means transformation of kinetic energy to internal energy in response to viscosity. Moreover, the heat conductivity enhances due to viscous dissipation for higher Br values. Consequently, the temperature increases. Figure 3(b) determines the Helmholtz-Smoluchowski velocity U_{HS} effect on θ. It indicates that θ declines for higher U_{HS}. Figure-3(c) examines that the temperature θ decreases against M. Figure-3(d) illustrates that the temperature θ increase of electro-osmotic parameter m. As a result, the decrease in EDL contributes to a remarkable increase for temperature θ. Figure-3(e) demonstrates that θ enhances while increase in value of Weissenberg number We. Result is compatible with previous analysis shown in references [35, 36].

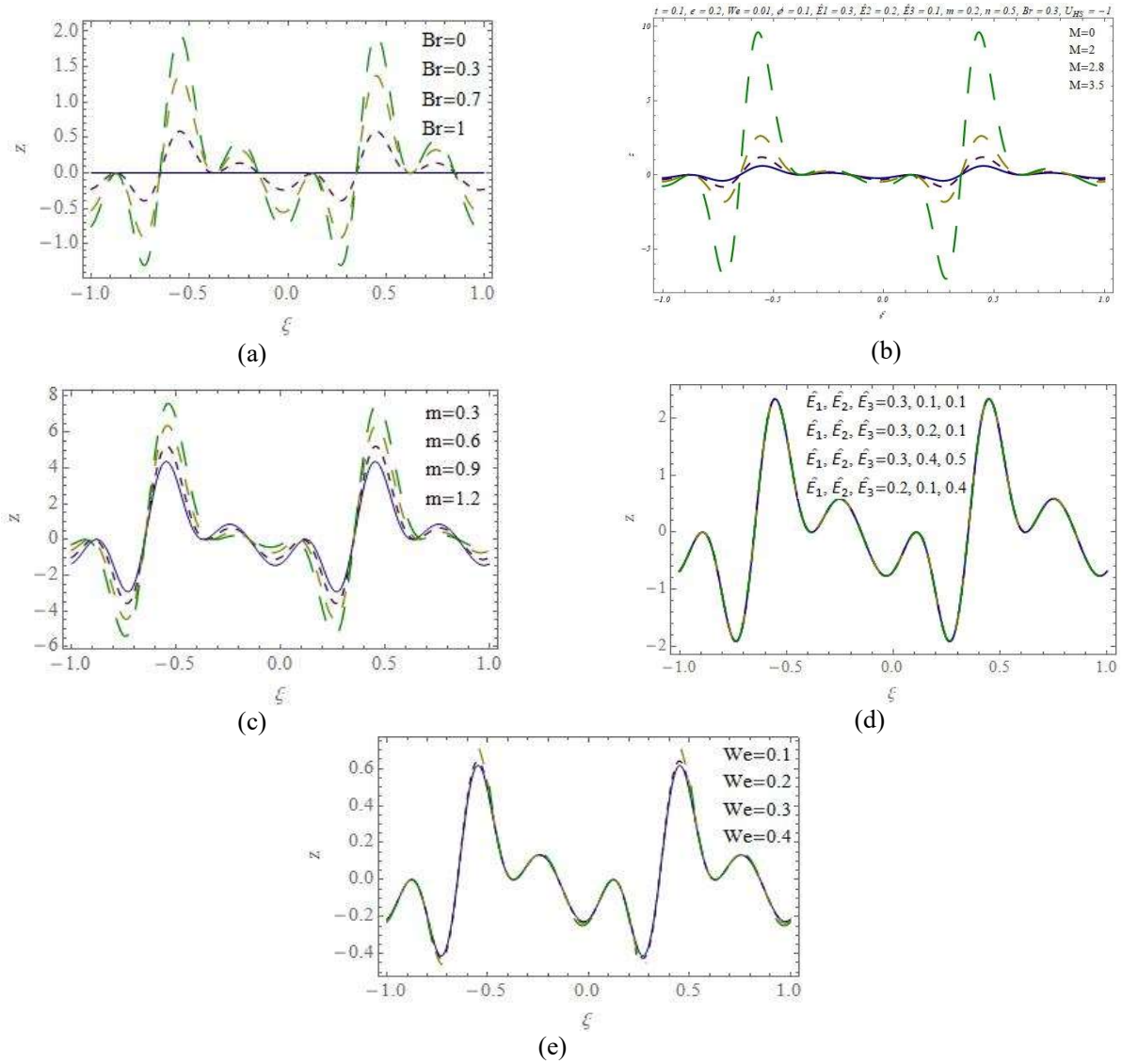

Figure 4. Coefficient of heat transfer z for (a). Br (b). M (c). m (d). $\hat{E}_1, \hat{E}_2, \hat{E}_3$ (e) We, while other parameters are $t = 0.1, \epsilon = 0.8, \phi = 0.1, \hat{E}_1 = 0.1, \hat{E}_2 = 0.2, \hat{E}_3 = 0.1, m = 0.2,\ n = 0.5, M = 0.3, We = 0.01, Br = 0.3,\ U_{HS} = -1.$

3.2. Coefficient of heat transfer

Electro-osmotic flow enables the coefficient of heat transfer to exhibit oscillating behavior through contraction and relaxation. The figures 4 ((a)−(e)) portray the coefficient of heat transfer z under impacts of Brinkmann number Br, Hartmann number M, electro-osmotic parameter m, wall parameters $\hat{E}_1, \hat{E}_2, \hat{E}_3$ and Weissenberg number We.

Figure-4(a) shows the rate of z in presence of stronger viscous dissipation effect i.e., the heat transfer rate increases for higher Brinkman number Br. Figure 4(b) indicates the decrease in z due to higher Hartman number M. The results shown in Figure-4(c) elucidates the increasing behavior in heat transfer rate for larger value of m. Figure 4(d) portrays that for ascending values of wall parameters $\hat{E}_1, \hat{E}_2, \hat{E}_3$ the coefficient of heat transfer decreases. Figure 4(e) demonstrates the gradual increasing behavior of z by higher We.

4. Conclusion

The article in hand presented the blood flow problem in microchannel via peristaltic wave train. Magnetic field is applied to linearize the flow field. Since imposed magnetic field tends to regulate the flow as it aids in

avoiding blood clots. Hence the magnetic field effect is seen increasing on velocity of flow. The velocity also shows increasing response towards rise in Weissenberg number and electro-osmotic parameter. The fast fluid particles also cause temperature rise and so it increases effectively with higher values of Weissenberg number, electro-osmotic parameter and Brinkman number. As Brinkman number demonstrates the internal heat generation that is why the temperature development is evident. Similar response for Hartmann number is seen for velocity and temperature of fluid. Since the flow is developed under peristaltic wave train at the channel walls so heat transfer rate at the channel boundary shows oscillatory behavior. The outcomes of this study are applicable in the field of medicine, biomedicine and also in industry where MHD with peristalsis has a promising role.

Nomenclature

a	Half width at inlet
b	Wave amplitude
λ	Wavelength
ξ, η	Axial, transverse coordinate
c	Wave velocity
t	Time
J	Current density
V	Velocity
e	Charge on electron
n	Fluid index
B_0	Magnetic field strength
σ	Electric conductivity of fluid
τ	Extra stress tensor
μ_∞	Infinite shear rate viscosity
μ_0	Zero shear rate viscosity
Π	Second invariant stress tensor
u	Axial velocity
v	Transverse velocity
p	Pressure
ρ	Fluid density
T	Temperature
k	Thermal conductivity
E_ξ	Axial electric current
ρ_e	Density of total ionic change
ε	Permittivity
n^+	Density numbers for cations
n^-	Density numbers for anions
T_1, T_0	Temperature on the top and bottom wall of micro channel
κ	Membrane elastic tension
l_1	Mass
D	Coefficient of viscous damping forces
δ	Wave number
Re	Reynolds number
ϵ	Amplitude ratio parameter
E_1 and E_2	Elastic variables
E_3	Damping variable
ψ	Stream function
M	Hartmann number
We	Weissenberg number
Pr	Prandtl number
E	Eckert number
Br	Brinkman number
Sc	Schmidt number
Pe	Ionic Peclet number
λ_d	Debye length

References

[1] N. Bag, S. Bhattacharyya, "Electroosmotic flow of a non-Newtonian fluid in a microchannel with heterogeneous surface potential," *Journal of Non-Newtonian Fluid Mechanics*, vol. 259, pp.48-60, Sep. 2018.

[2] S.U. Mamatha, R.R. Devi, N.A. Ahammad, N.A. Shah, B.M. Rao, C.S.K. Raju, M.I. Khan, K. Guedri, "Multi-linear regression of triple diffusive convectively heated boundary layer flow with suction and injection: Lie group transformations," *International Journal of Modern Physics B*, vol. *37*, No. 01, pp. 2350007, Jan. 2023.

[3] J. Akram, N.S. Akbar, D. Tripathi, "Electroosmosis augmented MHD peristaltic transport of SWCNTs suspension in aqueous media," *Journal of Thermal Analysis and Calorimetry*, vol. 147, pp.1-18, Feb. 2022.

[4] S. Hussain, N. Ali, "Electro-kinetically modulated peristaltic transport of multilayered power-law fluid in an

axisymmetric tube," *The European Physical Journal Plus*, vol. 135, No. 4, pp. 348, Apr. 2020.

[5] M.F. Ahmed, A. Zaib, F. Ali, O.T. Bafakeeh, E.S.M. Tag-ElDin, K. Guedri, S. Elattar, M.I. Khan, "Numerical computation for gyrotactic microorganisms in MHD radiative Eyring–Powell nanomaterial flow by a static/moving wedge with Darcy–Forchheimer relation," *Micromachines*, vol. *13*, No.10, pp.1768, Oct. 2022.

[6] M. Nazeer, F. Hussain, M.I. Khan, K. Khalid, "Theoretical analysis of electrical double layer effects on the multiphase flow of Jeffrey fluid through a divergent channel with lubricated walls," *Waves in Random and Complex Media*, pp.1-15, Sep. 2022.

[7] Zeeshan, A. Riaz, F. Alzahrani, "Electroosmosis-modulated bio-flow of nanofluid through a rectangular peristaltic pump induced by complex traveling wave with zeta potential and heat source," *Electrophoresis*, vol. *42,* No. 21-22, pp. 2143-2153, Nov. 2021.

[8] J. Akram, N.S. Akbar, D. Tripathi, "Analysis of electroosmotic flow of silver-water nanofluid regulated by peristalsis using two different approaches for nanofluid," *Journal of Computational Science*, vol. 62, pp. 101696, Jul. 2022.

[9] J. Akram, N.S. Akbar, "Mathematical modeling of Aphron drilling nanofluid driven by electroosmotically modulated peristalsis through a pipe," *Mathematical Modelling of Natural Phenomena*, vol. 17, No. 19, pp.19, Mar. 2022.

[10] E.N. Maraj, S.I. Shah, N.S. Akbar, T. Muhammad, "Thermally progressive Particle-Cu/Blood peristaltic transport with mass transfer in a Non-Uniform Wavy Channel: Closed-form exact solutions," *Alexandria Engineering Journal*, vol. 74, pp.453-466, Jul. 2023.

[11] J. Akram, N.S. Akbar, M. Alansari, D. Tripathi, "Electroosmotically modulated peristaltic propulsion of TiO2/10W40 nanofluid in curved microchannel," *International Communications in Heat and Mass Transfer*, vol. 136, pp. 106208, Jul. 2022.

[12] J. Akram, N.S. Akbar, D. Tripathi, "A theoretical investigation on the heat transfer ability of water-based hybrid (Ag–Au) nanofluids and Ag nanofluids flow driven by electroosmotic pumping through a microchannel," *Arabian Journal for Science and Engineering*, vol. 46, pp. 2911-2927, Mar. 2021.

[13] Zeeshan, N. Shehzad, M. Atif, R. Ellahi, S.M. Sait, "Electromagnetic flow of SWCNT/MWCNT suspensions in two immiscible water-and engine-oil-based Newtonian fluids through porous media," *Symmetry*, vol. 14, No. 2, pp. 406, Feb. 2022.

[14] Zeeshan, A. Riaz, F. Alzahrani, "Electroosmosis-modulated bio-flow of nanofluid through a rectangular peristaltic pump induced by complex traveling wave with zeta potential and heat source," *Electrophoresis*, vol. 42, No. 21-22, pp. 2143-2153, Nov. 2021.

[15] E.N. Maraj, N.S. Akbar, I. Zehra, A.W. Butt, H.A. Alghamdi, "Electro-osmotically modulated magneto hydrodynamic peristaltic flow of menthol based nanofluid in a uniform channel with shape factor." *Journal of Magnetism and Magnetic Materials*, vol. 576, pp. 170774, Jun. 2023.

[16] S. Saba, F.M. Abbasi, S.A. Shehzad, "Influence of curvature-dependent channel walls on MHD peristaltic flow of viscous fluid with Hall currents and Joule dissipation," *Scientia Iranica*, vol. *29*, No. 6, pp. 3107-3118, Dec. 2022.

[17] E.N. Maraj, I. Zehra, N. SherAkbar, "Rotatory flow of MHD (MoS2-SiO2)/H2O hybrid nanofluid in a vertical channel owing to velocity slip and thermal periodic conditions," *Colloids and Surfaces A: Physicochemical and Engineering Aspects*, vol. 639, pp. 128383, Apr. 2022.

[18] O.T. Bafakeeh, K. Raghunath, F. Ali, M. Khalid, E.S.M. Tag-ElDin, M. Oreijah, K. Guedri, N.B. Khedher, M.I. Khan, "Hall current and Soret effects on unsteady MHD rotating flow of second-grade fluid through porous media under the influences of thermal radiation and chemical reactions," *Catalysts*, vol. *12*, No. 10, pp. 1233, Oct. 2022.

[19] S. Li, M.I. Khan, F. Alzahrani, S.M. Eldin, "Heat and mass transport analysis in radiative time dependent flow in the presence of Ohmic heating and chemical reaction, viscous dissipation: An entropy modeling," *Case Studies in Thermal Engineering*, vol. *42*, pp.102722, Feb. 2023.

[20] L.A. Khan, M. Raza, N.A. Mir, R. Ellahi, "Effects of different shapes of nanoparticles on peristaltic flow of MHD nanofluids filled in an asymmetric channel: a novel mode for heat transfer enhancement," *Journal of Thermal Analysis and Calorimetry*, vol. 140, pp. 879-890, May. 2020.

[21] H.R. Patel, "Thermal radiation effects on MHD flow with heat and mass transfer of micropolar fluid between two vertical walls," *International Journal of Ambient Energy*, vol. 42, No. 11, pp. 1281-1296, Aug. 2021.

[22] K.V. Reddy, M.G. Reddy, "MHD thermal radiation and chemical reaction effects with peristaltic transport of the Eyring-Powell fluid through a porous medium," *Journal of Computational & Applied Research in Mechanical Engineering (JCARME)*, vol. 9, No. 1, pp. 89-105, Sep. 2019.

[23] G.C. Shit, S. Maiti, M. Roy, J.C. Misra, "Pulsatile flow and heat transfer of blood in an overlapping vibrating atherosclerotic artery: A numerical study," *Mathematics and Computers in Simulation*, vol. 166, pp. 432-450, Dec. 2019.

[24] Abbasi, W. Farooq, E.S.M. Tag-ElDin, S.U. Khan, M.I. Khan, K. Guedri, S. Elattar, M. Waqas, A.M. Galal, "Heat transport exploration for hybrid nanoparticle (Cu,

Fe3O4)—Based blood flow via tapered complex wavy curved channel with slip features," *Micromachines*, vol. 13*,* No. 9, pp. 1415, Aug. 2022.

[25] Y.K. Ha, H. Hong, E. Yeom, J.M. Song, "Numerical study of the pulsatile flow depending on non-Newtonian viscosity in a stenosed microchannel," *Journal of Visualization*, vol. 23, No. 1, pp. 61-70, Feb. 2020.

[26] H. Waqas, M. Oreijah, K. Guedri, S.U. Khan, S. Yang, S. Yasmin, M.I. Khan, O.T. Bafakeeh, E.S.M. Tag-ElDin, A.M. Galal, "Gyrotactic motile microorganisms impact on pseudoplastic nanofluid flow over a moving Riga surface with exponential heat flux," *Crystals*, vol. *12*, No. 9, pp. 1308, Sep. 2022.

[27] T. Hayat, R. Iqbal, A. Tanveer, A. Alsaedi, "Variable viscosity effect on MHD peristaltic flow of pseudoplastic fluid in a tapered asymmetric channel," *Journal of Mechanics*, vol. 34, No. 3, pp. 363-374, Jun. 2018.

[28] S. Noreen, S. Waheed, A. Hussanan, "Peristaltic motion of MHD nanofluid in an asymmetric micro-channel with Joule heating, wall flexibility and different zeta potential," *Boundary Value Problems*, No. 12, pp. 1-23, Dec. 2019.

[29] Tanveer, T. Hayat, A. Alsaedi, B. Ahmad, "Heat transfer analysis for peristalsis of MHD Carreau fluid in a curved channel through modified Darcy law," *Journal of Mechanics*, vol. 35, No. 4, pp. 527-535, Aug. 2019.

[30] M.M. Bhatti, R. Ellahi, A. Zeeshan, M. Marin, N. Ijaz, "Numerical study of heat transfer and Hall current impact on peristaltic propulsion of particle-fluid suspension with compliant wall properties," *Modern Physics Letters B*, vol. 33, No. 35, pp. 1950439, Dec. 2019.

[31] M. Gudekote, C. Rajashekhar, H. Vaidya, K.V. Prasad, O.D. Makinde, "Effects wall properties on peristaltic transport of Rabinowitsch fluid through an inclined Non-uniform slippery tube," *In Defect and Diffusion Forum,Trans Tech Publications Ltd.*, vol. 392, pp. 138-157, 2019.

[32] M. Gudekote, H. Vaidya, D. Baliga, C. Rajashekhar, K.V. Prasad, "The effects of convective and porous conditions on peristaltic transport of non-Newtonian fluid through a non-uniform channel with wall properties," *Journal of Advanced Research in Fluid Mechanics and Thermal Sciences*, vol. 63, No. 1, pp. 52-71, Nov. 2019.

[33] I.M. Eldesoky, R.M. Abumandour, M.H. Kamel, E.T. Abdelwahab, "The combined influences of heat transfer, compliant wall properties and slip conditions on the peristaltic flow through tube," *SN Applied Sciences*, vol. 1, No. 897, pp. 1-16, Aug. 2019.

[34] S. Noreen, S. Waheed, A. Hussanan, D. Lu, "Analytical solution for heat transfer in electro-osmotic flow of a Carreau fluid in a wavy microchannel," *Applied Sciences*, vol. 9, No. 20, pp. 43-59, Oct. 2019.

[35] T. Hayat, N. Aslam, M. Rafiq, F.E. Alsaadi, "Hall and Joule heating effects on peristaltic flow of Powell–Eyring liquid in an inclined symmetric channel," *Results in Physics*, vol. 7, pp. 518-528, Jan. 2017.

[36] T. Hayat, H. Zahir, A. Alsaedi, B. Ahmad, "Hall current and Joule heating effects on peristaltic flow of viscous fluid in a rotating channel with convective boundary conditions," *Results in Physics*, vol. 7, pp. 2831-2836, Jan. 2017.